



HAL
open science

Study of humic-like substances of dissolved organic matter using size exclusion chromatography and chemometrics

Sylvain Faixo, Romain Capdeville, Sofiane Mazeghrane, Mathieu Haddad, Gilberte Gaval, Etienne Paul, Florence Benoit-Marquié, Jean-Christophe Garrigues

► To cite this version:

Sylvain Faixo, Romain Capdeville, Sofiane Mazeghrane, Mathieu Haddad, Gilberte Gaval, et al.. Study of humic-like substances of dissolved organic matter using size exclusion chromatography and chemometrics. *Journal of Environmental Management*, 2024, 366, pp.121750. 10.1016/j.jenvman.2024.121750 . hal-04637966

HAL Id: hal-04637966

<https://hal.science/hal-04637966>

Submitted on 8 Jul 2024

HAL is a multi-disciplinary open access archive for the deposit and dissemination of scientific research documents, whether they are published or not. The documents may come from teaching and research institutions in France or abroad, or from public or private research centers.

L'archive ouverte pluridisciplinaire **HAL**, est destinée au dépôt et à la diffusion de documents scientifiques de niveau recherche, publiés ou non, émanant des établissements d'enseignement et de recherche français ou étrangers, des laboratoires publics ou privés.



Research article

Study of humic-like substances of dissolved organic matter using size exclusion chromatography and chemometrics

Sylvain Faix^{a,c}, Romain Capdeville^b, Sofiane Mazeghrane^a, Mathieu Haddad^d, Gilberte Gaval^a, Etienne Paul^c, Florence Benoit-Marquié^b, Jean-Christophe Garrigues^{b,*}^a SUEZ, Centre International de Recherche Sur l'Eau et l'Environnement (CIRSEE), 38 rue du Président Wilson, 78230, Le Pecq, France^b Laboratoire SOFTMAT (IMRCP), Université de Toulouse, CNRS UMR 5623, Université Paul Sabatier, 118 route de Narbonne, CEDEX 9, 31062, Toulouse, France^c TBI, Université de Toulouse, CNRS, INRAE, INSA, Toulouse, France, 135 avenue de Rangueil, CEDEX 04, 31077, Toulouse, France^d SUEZ Engineering & Construction, SUEZ International, Tour CB21, 16 place de l'Iris, La Défense, 92040, Paris, France

ARTICLE INFO

Handling editor: Dr. Lixiao Zhang

Keywords:

Melanoidin

Humic acid

Recalcitrant organic compound

Size exclusion chromatography

Fluorescence

Chemometrics

ABSTRACT

The study of dissolved organic matter (DOM) presents a significant challenge for environmental analyses and the monitoring of wastewater treatment plants (WWTPs). This is particularly true for the tracking of recalcitrant to biodegradation dissolved organic matter (rDOM) compounds, which is generated during the thermal pretreatment of sludge. This study aims to develop analytical and chemometric methods to differentiate melanoidins from humic acids (HAs), two components of rDOM that require monitoring at various stages of wastewater treatment processes due to their distinct biological effects. The developed method implements the separation of macromolecules through ultra-high-performance liquid chromatography size-exclusion chromatography (UHPLC SEC) followed by online UV and fluorescence detection. UV detection was performed at 210, 254, and 280 nm, and fluorescence detection at six excitation/emission pairs: 230/355 nm, 270/355 nm, 240/440 nm, 270/500 nm, 330/425 nm, and 390/500 nm. Chromatograms obtained for each sample from these nine detection modes were integrated and separated into four molecular fractions: >40 kDa, 20–40 kDa, 10–20 kDa, and <10 kDa. To enhance analytical resolution and normalize the data, ratios were calculated from the areas of chromatographic peaks obtained for each detection mode. The results demonstrate the utility of these ratios in discriminating samples composed of HAs, melanoidins, and their mixtures, through principal component analysis (PCA). Low molecular weight fractions were found to be specific to melanoidins, while high molecular weight fractions were characteristic of HAs. For the detection modes specific to melanoidins, UV absorbance at 210, 254, and 280 nm were predominantly present in the numerators, with tryptophan-like fluorescence emissions in the denominators. Conversely, fluorescence emissions largely represented both numerators and denominators for HAs. This online method also enables the discrimination of pseudo-melanoidins, compounds revealing a nitrogen deficiency in their chemical structures.

1. Introduction

Dissolved organic matter (DOM) is a complex matrix of diverse organic compounds ubiquitous in aquatic and terrestrial environments, playing a pivotal role in biological and geochemical processes (McDowell, 2023). Rivers are considered as 'channels' where organic matter interacts with soils and is transported to marine environments. During these transport phases, DOM constantly undergoes various physical, photochemical, and microbial degradation processes (Cai et al., 2023; Linnik et al., 2023). Rivers are also used as channels for drinking water

supply, and wastewater treatment systems discharge effluents into them. DOM is thus one of the primary indicators of water quality (Rodríguez-Vidal et al., 2021). DOM is a reservoir of carbon, nitrogen and other essential elements, significantly impacting ecological, environmental and biotechnological systems (Ma et al., 2001). Understanding the composition and dynamics of DOM is paramount to comprehend its role in nutrient cycling, carbon sequestration and overall ecosystem functioning. The major component of natural allochthonous DOM consists of humic compounds, characterized by relatively high aromaticity and molecular weight (Vogt et al., 2023; Lee and Park, 2022).

* Corresponding author.

E-mail address: jean-christophe.garrigues@univ-tlse3.fr (J.-C. Garrigues).<https://doi.org/10.1016/j.jenvman.2024.121750>

Received 12 March 2024; Received in revised form 26 June 2024; Accepted 3 July 2024

Available online 6 July 2024

0301-4797/© 2024 The Authors. Published by Elsevier Ltd. This is an open access article under the CC BY license (<http://creativecommons.org/licenses/by/4.0/>).

Conversely, autochthonous DOM is predominantly composed of fulvic material, which exhibits lower aromaticity and size (Egeberg et al., 1999). Furthermore, in most watercourses, there are anthropogenic inputs of DOM. These anthropogenic inputs of DOM consist of direct pollution, associated with the external introduction of DOM into the aquatic environment (Ifon et al., 2023). The term 'anthropogenic' in this context thus refers to local sources of DOM pollution, such as those originating from agriculture, aquaculture, industry (food, cellulose, chemicals, etc.), and more broadly from wastewater treatment processes (Zhang et al., 2021). In the specific field of wastewater treatment, understanding DOM is essential for monitoring treatment processes. These processes play a crucial role in wastewater depollution by preventing the discharge of anthropogenic pollutants into natural ecosystems (Kašanin-Grubin et al., 2019; Häder et al., 2020). The preservation of the environment and the prevention of issues such as eutrophication and chemical contamination are ensured through the enforcement of increasingly stringent discharge standards, such as chemical oxygen demand (COD) at 125 mg O₂ L⁻¹ and Total Nitrogen (TN) at 10–15 mg N L⁻¹ in Europe (Haileux, 2023). Most urban wastewater treatment plants (WWTP) employ biological processes to break down DOM and reduce the concentration of dissolved compounds and suspended solids. As a result of these processes, the primary waste generated consists of biomass known as sludge, which requires further treatment (Rajasulochana and Preethy, 2016).

The growing quantity of sludge produced by these treatment facilities poses a significant challenge in terms of both their operations and their environmental impact (Lu et al., 2019). Consequently, anaerobic digestion (AD) is implemented in various wastewater treatment plants to recover energy, reduce sludge volume, and stabilize biomass (Nabaterga et al., 2021). AD serves to decrease organic compounds, odours, and pathogens while generating biogas for electricity and heat production (Obileke et al., 2021). Pretreatment, particularly the hydrolysis step of AD, in an endeavour to enhance the accessibility of DOM for bacterial digestion, will bring about alterations in both its composition and the structure of chemical species in solution by introducing organic substances from the cellular organelles of the bacteria involved in the process (Tatla et al., 2024). Numerous pretreatment methods before AD have been developed to enhance hydrolysis efficiency and improve AD performance, including mechanical, thermal, chemical and biological treatments (Zhen et al., 2017). A recent innovation in wastewater treatment involves the use of thermal treatment to enhance sludge processing (Barber, 2016). This process entails heating the sludge to temperatures ranging from 140 to 200 °C, thereby increasing biogas production through anaerobic digestion and/or improving sludge dewaterability (Ariunbaatar et al., 2014). However, these thermal processes lead to the formation of significant quantities of soluble molecules that are not biologically degraded and are referred to as refractory dissolved organic matter (rDOM) (Devos et al., 2021). In addition to the rDOM formed during wastewater treatment processes, natural organic matter (NOM) is also found in surface waters and soils, and is likewise present in wastewater. Thus, the organic matter in wastewater samples consists of NOM, DOM, rDOM and biodegradable DOM (Yu et al., 2020). Regarding this organic matter in wastewater, the identification and quantification of rDOM pose an analytical challenge (Faixo et al., 2021). firstly, because thermal sludge treatment processes significantly increase the rDOM concentration in effluents by a factor of 100 compared to concentrations found in natural water or untreated wastewater (Hao et al., 2020), and secondly, due to the biological effects of the chemical compounds that make up rDOM (genotoxicity, cytotoxicity and antimicrobial activity) (Wang et al., 2011).

The rDOM compounds produced during thermal treatment steps are highly heterogeneous, and the specific reactivity conditions of the species present at high temperatures, as found in thermal processes (>120 °C), primarily generate high-molecular-weight polymers through Maillard reactions (Faixo et al., 2021). Two main families of macromolecules are gathered in humic-like species, which constitute the

rDOM. Humic acids (HAs) (Zheng et al., 2020) and melanoidins, then represent the greater part of rDOM found in the effluents of treated wastewater (Hao et al., 2020; Wang et al., 2011). Some studies show that thermal processes can alter the composition of rDOM, with an increase in the concentration of humic-like species. The physicochemical properties (hydrophobicity, aromaticity, molecular weight) of these families of compounds are different (Vogt et al., 2023) and will influence their behaviour during the treatment steps. It is therefore important to be able to discriminate between HAs and melanoidins for quality monitoring of discharges and for process monitoring to optimize them. The structure of HAs and melanoidins is highly complex and heterogeneous (Nebbioso and Piccolo, 2012; Rodríguez et al., 2015), which increases the challenges of specific characterization of each of these macromolecules.

Fluorescence spectroscopy has been widely used to analyse humic-like substances in DOM and wastewater (Rodríguez-Vidal et al., 2020). This technique provides information about the structure of humic substances: the intensity and position of fluorescence peaks can be correlated with certain structural properties of macromolecules, such as the number of carboxylic acid functions, the degree of humification, and aromaticity (Rodríguez et al., 2014). For this method, sample preparation is limited to simple filtration and pH adjustment for certain analytes. This technique allows for an initial level of discrimination between HAs and melanoidins through the study of excitation emission matrix spectra (EEMs). However, the close proximity of specific excitation/emission pairs (Ex/Em) for HAs and melanoidins can lead to spectral overlap between these two families. By coupling fluorescence detection and UV absorbance with size exclusion chromatography (SEC), it is possible to fractionate humic-like species and other macromolecular classes (various protein families) that make up DOM, but no definite discrimination has been observed between HAs and melanoidins (Faixo et al., 2021; Ignatev and Tuhkanen, 2019).

The objective of this study is to develop an easy-to-implement analytical methodology for future monitoring of wastewater treatment processes, enabling discrimination between samples composed mainly of melanoidins or humic acids, by integrating U-HPLC SEC separation, UV and fluorescence detection. To develop the method, standards of synthetic melanoidins and humic acids were analysed both pure and in mixture. To increase the number of analytical parameters, specific ratios were calculated between the areas of the detected peaks for different fractions separated by U-HPLC SEC, for UV and fluorescence detection modes, and the specific parameters of each species were identified through a chemometric approach.

2. Materials and methods

2.1. Chemicals

D-Glucose, glycine, sodium bicarbonate, humic acid, sodium phosphate monobasic dihydrate, sodium phosphate dibasic dihydrate, sodium hydroxide, hydrochloric acid solution 1.0 N, phosphorylase b, bovine serum albumin, albumin from chicken egg, pepsin, lysozyme from chicken egg and cytochrome c were purchased from Sigma-Aldrich Co. (St Quentin Fallavier, France). Ultrapure water were prepared using water purified with a Milli-Q purification system (Millipore, St Quentin Yvelines, France).

2.2. Samples

2.2.1. Melanoidins

Synthetic melanoidins were prepared in accordance with Bernardo et al. (1997) for species synthesis under equimolar conditions between glucose and glycine. Melanoidins with a 1:1 M ratio of glucose and glycine were obtained by mixing 4.5 g (0.025 mol) of glucose, 1.88 g (0.025 mol) of glycine, and 0.42 g (0.005 mol) of sodium bicarbonate in 100 mL of ultrapure water. The 1:2 M fraction was obtained by mixing 4.5 g (0.025 mol) of glucose, 3.76 g (0.05 mol) of glycine, and 0.42 g

(0.005 mol) of sodium bicarbonate in 100 mL of ultrapure water. The 2:1 M fraction was obtained by mixing 8 g (0.05 mol) of glucose, 1.88 g (0.05 mol) of glycine and 0.42 g (0.005 mol) of sodium bicarbonate in 100 mL of ultrapure water. All mixtures were refluxed for 7 h at 95 °C with a magnetic stirrer (50 rpm). After being heated, the solutions were brought to room temperature, then lyophilized to remove water and stored at 3 °C. A stock solution of each synthetic melanoidin 1:1, 1:2, and 2:1, was prepared by adding 40 mg of lyophilized powder to 1 mL of ultra-pure water in a microtube. Subsequently, dilutions of 1/10, 1/50, 1/100, 1/250 and 1/500 were made in ultra-pure water, corresponding to mass concentrations of 4, 0.8, 0.4, 0.16, and 0.08 mg. mL⁻¹, respectively, before analysis.

2.2.2. Humic acids

A stock solution was prepared by adding 40 mg of humic acid, 800 µL of ultra-pure water and 100 µL of 0.1 M sodium hydroxide to a microtube (1.5 mL, Eppendorf microcentrifuge tubes). The microtube was placed in an ultrasonic bath (Branson Ultrasonics bath, 1.9 L) for 30 min to achieve complete dissolution of the mixture. After dissolution, any residual sodium hydroxide was neutralized by adding 100 µL of 10⁻² M hydrochloric acid and this stock solution was stored at 3 °C until use. Dilutions of 1/10, 1/50, 1/100, 1/250 and 1/500 were made in ultra-pure water, corresponding to mass concentrations of 4, 0.8, 0.4, 0.16 and 0.08 mg. mL⁻¹, respectively, before analysis.

2.2.3. Melanoidins/HAs mixtures

Mixtures of each melanoidin (1:1, 1:2 and 2:1) and HAs were prepared. The 9/1 weight-to-weight proportion mixture was obtained by taking 900 µL from the 1/10 dilution of melanoidins and adding 100 µL from the 1/10 dilution of HA. The 1/1 mixture is obtained by taking 500 µL of melanoidins and adding 500 µL of the 1/10 HA solution, while the 1/9 mixture is obtained by taking 100 µL of melanoidins and adding 900 µL of the 1/10 HA solution. These mixtures are prepared before each analysis.

2.2.4. Digested sludge

A representative sample of the produced rDOM in a wastewater treatment plant was provided by Suez company. It consisted of leachate from digested sludge after hydrothermal carbonization (HTC) at 200 °C. 100 mL of this leachate was lyophilized. 40 mg of the powder was added to 1 mL of ultrapure water for analysis.

2.3. Size exclusion chromatography (SEC)

SEC was used to separate melanoidins and HAs based on their respective hydrodynamic volumes. The separation utilized a 4.6 mm × 150 mm Acquity UPLC Protein BEH SEC column with 125 Å pore size packed with 1.7 µm porous hybrid silica beads (Waters). The separation procedure was carried out using an Acquity UPLC system (Waters). The eluent phase consisted of a 7.5 mM phosphate buffer, pH 7.4, prepared with 140 mg sodium phosphate monobasic dihydrate, 500 mg sodium phosphate dibasic dihydrate and 500 mL of ultrapure water, filtered through 47 mm, 0.45 µm nylon membrane discs (Waters). The column oven temperature was set at 30 °C, the flow rate at 0.3 mL. min⁻¹, and the injection volume at 5 µL. All samples were filtered before injection with 13 mm, 0.2 µm nylon membrane syringe filters (Waters). Detection was carried out using an Acquity photodiode array (PDA) and Acquity fluorescence detectors (Waters). The selected wavelengths for detection and integration are provided in Table 1. All analyses were monitored using Empower 3 software (Waters), and all samples were analysed in triplicate to calculate the coefficient of variation for peak areas and retention times, which should not exceed 3.5 %. The column was calibrated by injecting a mixture (5 mg. mL⁻¹ each) of phosphorylase b (MW: 97.2 kDa), bovine serum albumin (MW: 66 kDa), albumin from chicken egg (MW: 44.2 kDa), pepsin (MW: 35 kDa), lysozyme from chicken egg (MW: 14.3 kDa) and cytochrome c (MW: 12.3 kDa).

Table 1

UV wavelengths and fluorescence Ex/Em pairs used for the integration of U-HPLC-SEC chromatograms with target chemical families and specificities.

UV wavelength (nm)	Code	Chemical family	Specificity
210	210	All	C sp ²
254	254	All	Aromaticity
280	280	Aromatic amino acids	Tryptophan, tyrosine
Ex/Em (nm)			
230/355	TRY1	Proteins	Tryptophan
270/355	TRY2	Proteins	Tryptophan
240/440	FA1	Humic like	Fulvic acids
270/500	FA2	Humic like	Fulvic acids
330/425	MEL	Humic like	Melanoidins
390/500	HA	Humic like	HAs

2.4. Chemometrics

2.4.1. Analytical database

Each chromatogram was integrated for all UV wavelengths and Ex/Em pairs (see Table 1). The peak areas were then grouped into four fractions (see Fig. S1, supplementary data): >40 kDa (F₁), 20–40 kDa (F₂), 10–20 kDa (F₃), and <10 kDa (F₄). From the integrated areas for each fraction, ratios were calculated using the following formula:

$$\text{Ratio} \frac{DM1}{DM2} F_n = \frac{\text{Integrated peak area fraction } F_n \text{ for } DM1}{\text{Integrated peak area fraction } F_n \text{ for } DM2}$$

With: DM1 = Detection mode 1

DM2 = Detection mode 2

F_n = Fraction number (from 1 to 4)

Each chromatogram was thus transformed into 144 analytical data points and all data of the analytical database were normalized by dividing each variable by the greatest value of the column.

2.4.2. Principal component analysis (PCA)

PCA was conducted by using the transformation of variables to describe the variance of the matrix, projecting them onto different components. Eigenvectors represented each variable in a correlation matrix for all components, and the samples corresponding to different dilutions of synthetic melanoidins and AHs, or mixtures, could be plotted on the corresponding score plot. PCAs were performed in MATLAB R2023b, with the statistics toolbox V.23.0, using, for each analysed sample, the 144 calculated analytical ratios. From all the components of the correlation matrices, two or three from PC1, PC2 and PC3 were included in the analyses to perform the classification of the samples, and 2D or 3D plots were defined to represent the correlation score.

3. Results and discussion

3.1. U-HPLC SEC separation of synthetic melanoidins and HAs

The preparation of synthetic melanoidins, which are used as standards for structural or compositional analysis, has been described (Cämmerer et al., 2002; Echavarría et al., 2012). The Maillard reaction that occurs at high temperatures involves the condensation between the amine function of an amino acid or a protein and the carbonyl function of a reducing sugar in basic conditions (Hidalgo et al., 1999). Various melanoidin standards were synthesized by varying the Glucose/Glycine molar ratio in proportions of 1:1, 1:2, and 2:1 to obtain macromolecules with diverse structures in which reactivity conditions are optimal (1:1 ratio), deficient in amine (2:1 ratio), or deficient in reducing sugar (1:2 ratio). After the synthesis step, all samples exhibit an intense brown coloration, as described in the literature (Mohsin et al., 2018).

Fig. 1 shows the UHPLC SEC chromatograms obtained with standard melanoidins (a) and HAs (b), for the specific Ex/Em pairs of each species: 380/425 nm for melanoidins and 390/500 nm for HAs.

For the synthetic melanoidins, the chromatogram (Fig. 1 (a)) shows separation of fractions in the 1–66 kDa range, with molar fractions in the 1–12 kDa range showing significant fluorescence intensity (>0.5 normalized fluorescence unit (FU)). For humic acids, there are three fractions between 66 and 18 kDa, followed by less well-resolved fractions down to 1 kDa. In the 1–12 kDa range, the fluorescence intensity is low (<0.25 normalized FU). The fractionation of HAs by SEC (Fig. 1 (b)) is complex due to the structural polydispersity. The commercial standards of HA analysed, produced from soils and surface water, may contain species with very high molecular weights (>300 kDa) (Christl et al., 2000). Depending on the origin and sample preparation chosen, the observed molecular weight limit decreases, ranging from 10 kDa to 20 kDa (Her et al., 2003; Perminova et al., 2003). There is a relationship between molecular weight, aromaticity and hydrophobicity of HAs. High molecular weight fractions exhibit an increase in aromaticity and hydrophobicity, enhancing hydrophobic interactions among these species, leading to the formation of insoluble aggregates (Gao et al., 2022). A dedicated sample preparation is then necessary to observe them, especially by controlling the pH. In samples from leachates of sludge from thermal treatment processes, these insoluble aggregates are not found in the soluble fraction of the DOM and are not sought. The HAs and melanoidins have shown fluorescence spectra over a wide range of wavelengths: Ex/Em 330–350/420–480 nm, depending on the sample origin and their molecular structure (Leenheer and Croue, 2003). Longer wavelengths are associated with increased aromaticity and conjugation of macromolecules (Dwyer et al., 2008; Coble, 1996). In this study, we selected the Ex/Em pair 330/425 nm for melanoidins and the Ex/Em pair 390/500 nm for HAs. Overlaying the separation performance of synthetic melanoidins and HAs with the chromatograms obtained under the same conditions for digested sludge samples, with specific fluorescence detection for melanoidins (Fig. 1 (c)) and HAs (Fig. 1 (d)), reveals that the majority of fractions found in these samples are within the 97–1 kDa range. The absorption and fluorescence emission specificities of melanoidins and HAs are related to their structure and vary depending on their sources (agro-food, soil, wastewater, sludge after thermal

treatment).

3.2. U-HPLC SEC separation of mixture composed of synthetic melanoidins and HAs

The analysis of mixtures consisting of synthetic melanoidins and HAs at different weight-to-weight proportions (Fig. 2) shows an evolution of the U-HPLC SEC chromatograms from samples predominantly composed of melanoidins (Fig. 2 (a)) to those mainly composed of HAs (Fig. 2 (c)).

To categorize the samples based on their melanoidin and HAs compositions, we grouped the molar fractions into four classes: >40 kDa, 20–40 kDa, 10–20 kDa, <10 kDa (Fig. S1, supplementary data). Each chromatogram was integrated at three UV absorbance wavelengths (210, 254 and 280 nm) and six fluorescence Ex/Em pairs (230/355 nm, 270/355 nm, 240/440 nm, 270/500 nm, 330/425 nm and 390/500 nm), with each detection mode being specific to a class of molecule or chemical bonds, as presented in Table 1.

3.3. Chemometrics

For each sample, the integrated peak areas in the nine detection modes from Table 1 are grouped into 4 M fractions (Fig. S1, supplementary data). To complete this table, ratios are calculated between the different detection modes, as presented in Table S1 (Supplementary data). For each sample, it is possible to calculate 144 ratios. The calculation of analytical ratios for DOM characterization was initially introduced with SUVA₂₅₄ to determine the aromaticity of a sample while accounting for variations in the amount of DOM (Dobbs et al., 1972). In the present study, a ratio, or its inverse, allows for the normalization of measurements by accounting for the species specifically determined by the detection mode of the denominator.

By integrating these ratios into a PCA (Fig. 3), it can be observed that the samples of synthetic melanoidins and HAs are positioned in two distinct zones, particularly well discriminated by Component 1, representing 31% of the variance. Melanoidins obtained with different ratios of glucose and glycine are discriminated by PC2, which represents 19% of the variance, and PC3 (9 %). In contrast to this specific melanoidin zone, the various dilutions of HAs are found, and between these two

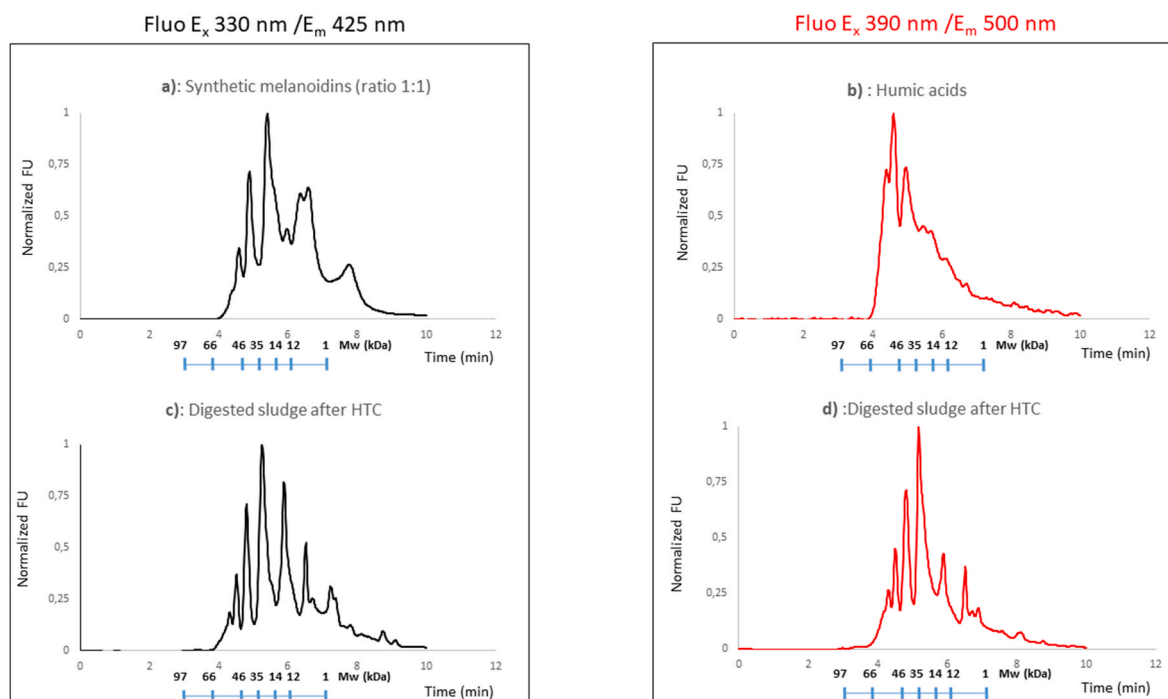


Fig. 1. U-HPLC SEC chromatograms of synthetic melanoidins (1:1) a), HAs b) and digested sludge c-d) with fluorescence detection.

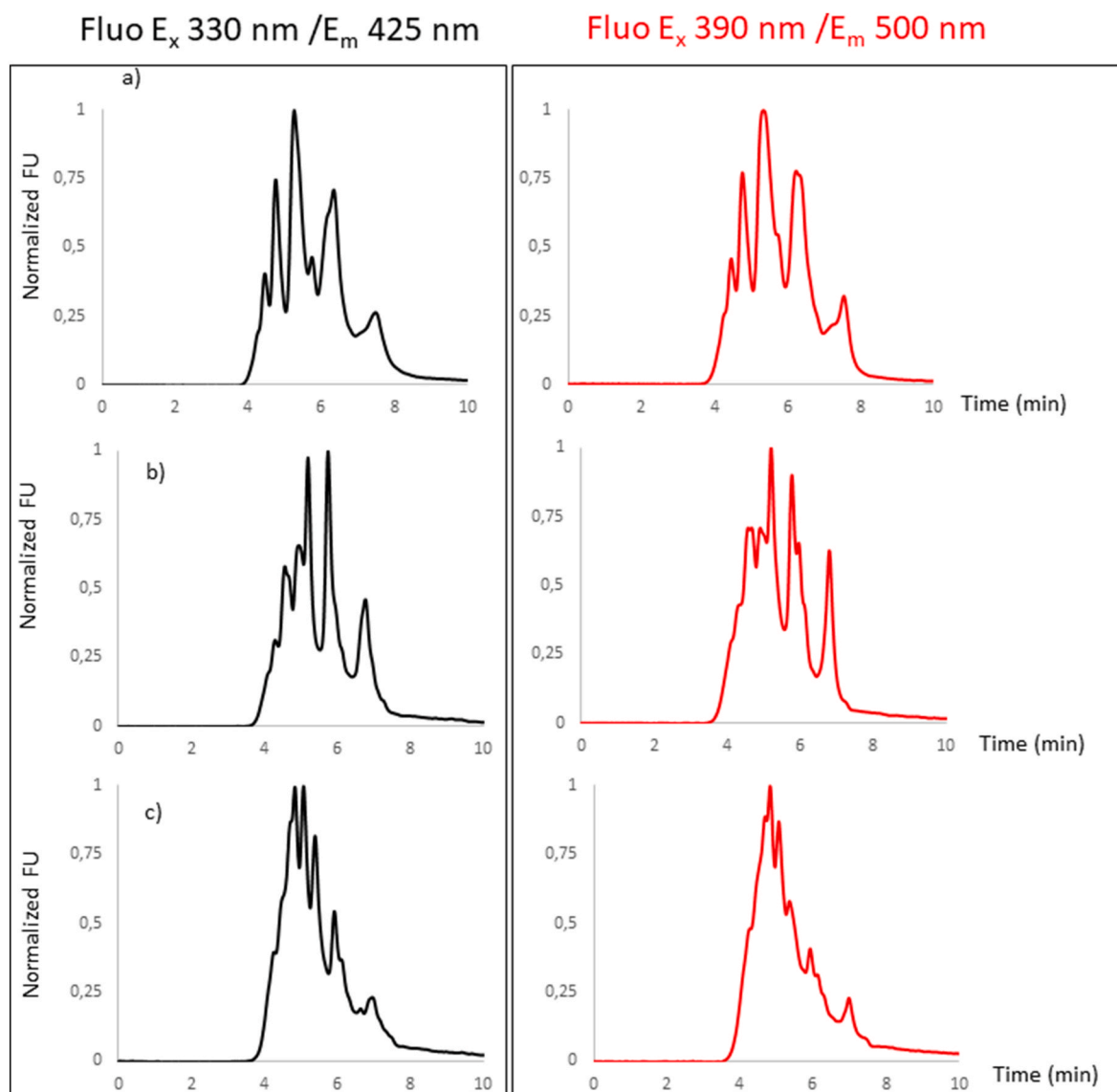


Fig. 2. U-HPLC SEC chromatograms of a mixture of synthetic melanoidins and HAs with fluorescence detection in the following weight-to-weight proportions: 9/1 (a); 1/1 (b); and 1/9 (c).

areas, there are mixtures consisting of different mass proportions of melanoidins and HAs. In particular, mixtures rich in melanoidins are predominantly oriented towards the melanoidin zone, while those rich in HAs are positioned in the zone of pure HA standards.

Taking a closer look at melanoidins and HAs separately (Fig. 4), it becomes evident that Component 1 (PC1), representing 44% of the variance, discriminates these two compound families using the ratios of different detection modes calculated for each of the 4 M mass fractions of the peaks separated by the U-HPLC SEC method. Table 2 shows that, for PC1, the eigenvalues with the highest absolute values, extracted from the vectors describing the variance of the analytical parameters of synthetic melanoidin samples in the PCA space, are all associated with molar fractions < 10 kDa (PC1 column, eigenvalues from -0.159 to -0.113). For HAs, the specific eigenvalues are associated with higher molar fractions: > 40 kDa, 10–20 kDa, or 20–40 kDa (PC1 column, eigenvalues from 0.167 to 0.124).

Regarding the ratios explaining the specific variance of melanoidin samples, UV absorbance's at 210, 280 and 254 nm are predominantly present in the numerator, associated with mainly TRY1 or TRY2 fluorescence emissions in the denominator. For the ratios explaining the specific variance of HA samples, the numerator is mainly related to

fluorescence emissions, particularly FA2, and the denominator is shared between MEL and HAs fluorescence emissions.

The discrimination of melanoidins and HA species by the UV absorbance at 280 nm, which is specific to $\pi - \pi^*$ transitions in the C=C bond, may indicate a difference in the number of heterocycles in the chemical families for each of the considered molar fractions (Mohsin et al., 2019). These two specific absorbances, normalized by TRY or MEL fluorescence emissions in two regions of low or high E_m/E_x wavelengths (Table 1), allow for the quantification of these heterocycles under these normalized conditions and enables the discrimination of the chemical species studied. For HAs, the numerators of the ratios, predominantly containing FA2, are specific to more pronounced conjugations for this class of molecules. For PC2, (Fig. 4, (a)), there is a distribution of synthetic melanoidin samples that positions in the same negative region of eigenvalues, the standards synthesized in excess of glucose (MEL 2:1), and those in excess of glycine (MEL 1:2). However, for PC3, (Fig. 4 (b)), it appears to be a distribution of the three standards following a binary separation that follows the nitrogen on carbon (N/C) ratio. The MEL 1:1 samples are positioned in the centre of PC3 (between -0.5 and 0) for $N/C = 1$. The MEL 2:1 samples are positioned towards 1.5 for $N/C < 1$, corresponding to structures with excess of carbon and MEL 1:2 towards

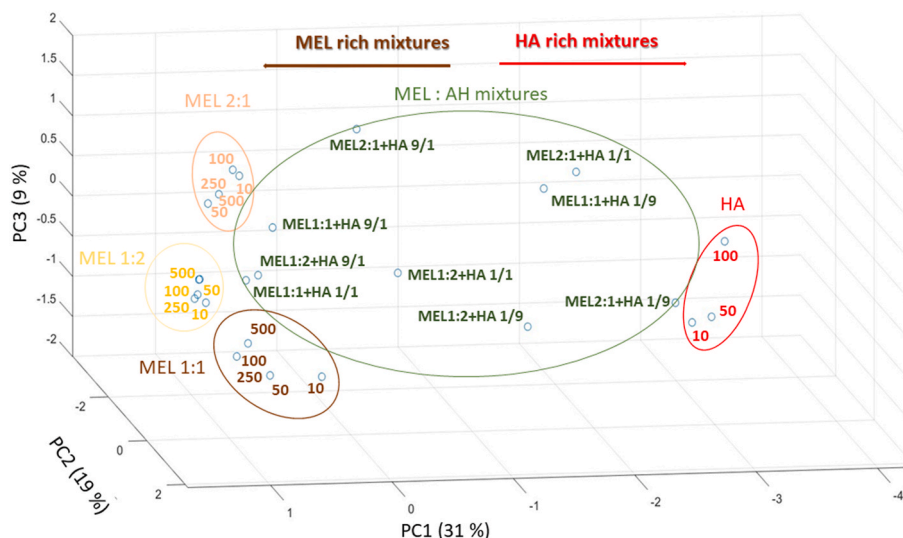


Fig. 3. PCA based on samples of synthetic melanoidin standards (MEL) synthesized at molar ratios 1:1, 2:1, 1:2 and dilution of 1/10 (10) to 1/500 (500); HAs at dilutions of 1/10 (10) to 1/100 (100); and MEL/HA mixtures (MEL:HA) at weight-to-weight proportions 9/1, 1/1 and 1/9.

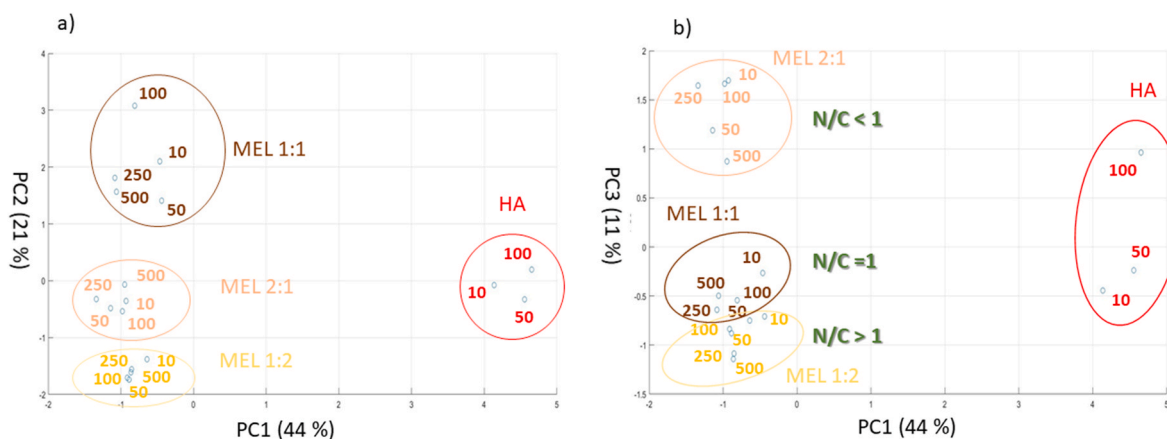


Fig. 4. 2D-PCA with PC1 and PC2 (a) or PC1 and PC3 (b) based on samples of synthetic melanoidin standards (MEL) synthesized at molar ratios 1:1, 2:1, 1:2 and dilution of 1/10 (10) to 1/500 (500); HA at dilutions of 1/10 (10) to 1/100 (100).

Table 2

Key eigenvalues and corresponding calculated analytical ratios for each of the principal components PC1, PC2 and PC3.

PC1		PC2		PC3	
Calculated ratio	Eigenvalue	Calculated ratio	Eigenvalue	Calculated ratio	Eigenvalue
210/280_<10 kDa	-0.159	TRY2/FA2_>40 kDa	-0.167	FA1/MEL_10-20 kDa	-0.232
280/TRY1_<10 kDa	-0.146	FA1/FA2_>40 kDa	-0.141	FA1/MEL_<10 kDa	-0.191
210/MEL_<10 kDa	-0.141	FA1/FA2_<10 kDa	-0.109	FA1/FA2_10-20 kDa	-0.153
210/TRY1_<10 kDa	-0.137	FA1/MEL_<10 kDa	-0.107	FA1/FA2_<10 kDa	-0.089
210/254_<10 kDa	-0.130	TRY1/FA2_>40 kDa	-0.091	254/FA1_>40 kDa	-0.082
280/FA2_<10 kDa	-0.127	210/TRY1_<10 kDa	-0.085	210/FA1_>40 kDa	-0.072
280/MEL_<10 kDa	-0.123	TRY2/HA_>40 kDa	-0.083	254/280_10-20 kDa	-0.071
280/TRY2_<10 kDa	-0.122	210/254_<10 kDa	-0.082	254/TRY2_>40 kDa	-0.069
254/TRY2_<10 kDa	-0.116	FA1/MEL_20-40 kDa	-0.075	254/TRY1_>40 kDa	-0.067
210/TRY2_<10 kDa	-0.113	FA1/HA_>40 kDa	-0.066	TRY2/FA1_>40 kDa	-0.067
TRY2/MEL_>40 kDa	0.124	280/FA1_20-40 kDa	0.131	280/HA_<10 kDa	0.149
280/HA_>40 kDa	0.130	280/FA1_<10 kDa	0.150	254/FA2_<10 kDa	0.152
FA2/MEL_>40 kDa	0.132	210/MEL_>40 kDa	0.172	280/FA1_10-20 kDa	0.153
280/MEL_>40 kDa	0.133	254/FA2_>40 kDa	0.177	FA1/FA2_20-40 kDa	0.154
FA2/HA_20-40 kDa	0.136	210/TRY1_>40 kDa	0.183	210/FA1_10-20 kDa	0.166
FA2/HA_10-20 kDa	0.139	210/FA2_>40 kDa	0.187	210/HA_<10 kDa	0.195
FA2/MEL_20-40 kDa	0.144	210/HA_>40 kDa	0.192	MEL/HA_<10 kDa	0.213
TRY1/MEL_>40 kDa	0.147	254/FA1_>40 kDa	0.199	280/FA1_<10 kDa	0.216
TRY1/HA_>40 kDa	0.148	254/TRY2_>40 kDa	0.208	MEL/HA_10-20 kDa	0.229
FA1/MEL_>40 kDa	0.167	280/TRY2_>40 kDa	0.217	210/FA1_<10 kDa	0.258

PC3 = -1 for N/C > 1, corresponding to structures with excess of nitrogen. There seems to be a correlation between the N/C ratio of synthetic melanoidins and the projection onto PC3 of the analytical ratios. For PC3, the molar fractions of the ratios with the highest eigenvalues in absolute value are found in low molar masses (<10 kDa and 10–20 kDa). For N/C ratios >1, the three highest eigenvalues in absolute value (-0.232 to -0.153, Table 2, PC3) are associated with calculated analytical ratios containing FA1 in the numerator and MEL or FA2 in the denominator. In contrast, for melanoidins synthesized in excess of carbon (N/C < 1), the numerator contains 210, 280 and MEL fluorescence emissions for the 3 highest eigenvalues (0.258–0.216, Table 2, PC3) and the denominators are composed of FA1 or HA.

It appears that for synthetic melanoidins formed in excess of glucose (N/C < 1), the fluorescence intensities at 210 nm and 280 nm, or a melanoidin fluorescence emission (Ex/Em: 330/425 nm) in the calculated ratios, explain the variance of these samples. In contrast, for synthetic melanoidins with N/C > 1, the calculated ratios involve FA1 (Ex/Em: 240/440). Our results can be related to those of Usman et al. (2020), who demonstrated that melanoidins with N/C < 1, referred to as pseudo-melanoidins, exhibit a higher number of pyrazine motifs and fewer conjugated sites compared to melanoidins formed in excess of nitrogen. Thus, in Fig. 4 (b), melanoidins with N/C > 1 are associated with specific FA1 fluorescence ratios, while the same species with N/C < 1 (Fig. 4 (a)) are associated with UV ratios at 210 nm and 280 nm, with less pronounced influence of fluorescence emissions. For these two classes of melanoidins, the ratios are normalized by fluorescence emissions at wavelengths higher than the numerators to discriminate between aromatic sites and more conjugated motifs generating these fluorescences. These results demonstrate the potential to synthesize melanoidins with different structures based on the initial N/C ratio conditions and the production of macromolecules that incorporate these differences.

4. Conclusion

In this study, a comprehensive methodology was developed for discriminating between samples composed of synthetic melanoidins and HAs in DOM through the integration of U-HPLC SEC separation, UV, and fluorescence detection. The application of PCA allowed for a detailed exploration of sample variance, demonstrating that the dilutions of each species did not compromise the specificity of the method. A key aspect of this methodology was the calculation of specific ratios across three UV detection modes and six fluorescence modes, which enhanced the depth of information extracted from each sample by normalising values with varied numerators.

The results indicated a clear discrimination between melanoidins and HAs, with samples predominantly positioning within the PCA domain space corresponding to their major components. The study's findings suggest that the integration of UV and fluorescence detection with U-HPLC SEC, combined with chemometric analysis, provides a robust framework for distinguishing complex mixtures of synthetic melanoidins and HAs in DOM. The discrimination reveals different absorbance and fluorescence properties for the two classes of rDOM, associated with high molecular weight fractions for HAs and lower molecular weight fractions for melanoidins.

This analytical method was applied to the study of commercial standards of HAs, synthetic melanoidins, and a representative sample from a leachate from digested sludge after hydrothermal carbonization.

CRedit authorship contribution statement

Sylvain Faix: Writing – original draft, Resources, Investigation. **Romain Capdeville:** Resources, Methodology. **Sofiane Mazeghrane:** Writing – original draft, Resources, Methodology. **Mathieu Haddad:** Writing – review & editing, Writing – original draft, Resources, Methodology. **Gilberte Gaval:** Writing – original draft, Resources,

Methodology. **Etienne Paul:** Writing – review & editing, Writing – original draft, Validation, Supervision, Project administration. **Florence Benoit-Marquié:** Writing – original draft, Resources, Methodology. **Jean-Christophe Garrigues:** Writing – review & editing, Writing – original draft, Validation, Formal analysis, Conceptualization.

Declaration of competing interest

The authors declare that they have no known competing financial interests or personal relationships that could have appeared to influence the work reported in this paper.

Data availability

Data will be made available on request.

Acknowledgements

The authors would like to thank the SUEZ group for its scientific contribution and financial support for this study. Grant# CT REFRACTO SUEZ-IMRCP.

Appendix A. Supplementary data

Supplementary data to this article can be found online at <https://doi.org/10.1016/j.jenvman.2024.121750>.

References

- Ariunbaatar, J., Panico, A., Esposito, G., Pirozzi, F., Lens, P.N.L., 2014. Pretreatment methods to enhance anaerobic digestion of organic solid waste. *Appl. Energy* 123, 143–156. <https://doi.org/10.1016/j.apenergy.2014.02.035>.
- Barber, W.P.F., 2016. Thermal hydrolysis for sewage treatment: a critical review. *Water Res.* 104, 53–71. <https://doi.org/10.1016/j.watres.2016.07.069>.
- Bernardo, E.C., Egashira, R., Kawasaki, J., 1997. Decolorization of molasses' wastewater using activated carbon prepared from cane bagasse. *Carbon* N. Y. 35, 1217–1221. [https://doi.org/10.1016/S0008-6223\(97\)00105-X](https://doi.org/10.1016/S0008-6223(97)00105-X).
- Cai, T., Zhang, X., Zhang, S., Ming, Y., Zhang, Q., 2023. Photochemical behaviors of dissolved organic matter in aquatic environment: Generation, characterization, influencing factors and practical application. *Environ. Res.* 231 <https://doi.org/10.1016/j.envres.2023.116174>.
- Cämmerer, B., Jalyschko, W., Kroh, L.W., 2002. Intact carbohydrate structures as part of the melanoidin skeleton. *J. Agric. Food Chem.* 50, 2083–2087. <https://doi.org/10.1021/jf011106w>.
- Christl, I., Knicker, H., Kögel-Knabner, I., Kretzschmar, R., 2000. Chemical heterogeneity of humic substances: characterization of size fractions obtained by hollow-fibre ultrafiltration. *Eur. J. Soil Sci.* 51, 617–625. <https://doi.org/10.1111/j.1365-2389.2000.00352.x>.
- Coble, P.G., 1996. Characterization of marine and terrestrial DOM in seawater using excitation-emission matrix spectroscopy. *Mar. Chem.* 51, 325–346. [https://doi.org/10.1016/0304-4203\(95\)00062-3](https://doi.org/10.1016/0304-4203(95)00062-3).
- Devos, P., Haddad, M., Carrère, H., 2021. Thermal hydrolysis of municipal sludge: Finding the temperature Sweet Spot: a review. *Waste and Biomass Valorization* 12, 2187–2205. <https://doi.org/10.1007/s12649-020-01130-1>.
- Dobbs, R.A., Wise, R.H., Dean, R.B., 1972. The use of ultra-violet absorbance for monitoring the total organic carbon content of water and wastewater. *Water Res.* 6, 1173–1180. [https://doi.org/10.1016/0043-1354\(72\)90017-6](https://doi.org/10.1016/0043-1354(72)90017-6).
- Dwyer, J., Starrenburg, D., Tait, S., Barr, K., Batstone, D.J., Lant, P., 2008. Decreasing activated sludge thermal hydrolysis temperature reduces product colour, without decreasing degradability. *Water Res.* 42, 4699–4709. <https://doi.org/10.1016/j.watres.2008.08.019>.
- Echavarría, A.P., Pagán, J., Ibarz, A., 2012. Melanoidins formed by Maillard reaction in food and their biological activity. *Food Eng. Rev.* 4, 203–223. <https://doi.org/10.1007/s12393-012-9057-9>.
- Egeberg, P.K., Gjessing, E.T., Ratnaweera, H., Moghissi, A.A., 1999. Natural organic matter: Editorial. *Environ. Int.* 25, 143–144. [https://doi.org/10.1016/S0160-4120\(98\)00120-2](https://doi.org/10.1016/S0160-4120(98)00120-2).
- Faix, S., Gehin, N., Balayssac, S., Gilard, V., Mazeghrane, S., Haddad, M., Gaval, G., Paul, E., Garrigues, J.-C., 2021. Current trends and advances in analytical techniques for the characterization and quantification of biologically recalcitrant organic species in sludge and wastewater: a review. *Anal. Chim. Acta* 1152. <https://doi.org/10.1016/j.aca.2021.338284>.
- Gao, R., Cui, K., Liang, W., Wang, H., Wei, S., Zhou, Y., Zeng, F., 2022. Molecular weight-dependent adsorption heterogeneities of humic acid on microplastics in aquatic environments: further insights from fluorescence spectra combined with two-dimensional correlation spectroscopy and site energy distribution analysis. *J. Environ. Chem. Eng.* 10 <https://doi.org/10.1016/j.jece.2022.108948>.

- Häder, D.P., Banaszak, A.T., Villafañe, V.E., Narvarte, M.A., González, R.A., Helbling, E. W., 2020. Anthropogenic pollution of aquatic ecosystems: Emerging problems with global implications. *Sci. Total Environ.* 713 <https://doi.org/10.1016/j.scitotenv.2020.136586>.
- Haillex, V., 2023. Urban wastewater treatment: Updating EU rules. *Brief*, 739370 (2024) 1–12. https://www.europarl.europa.eu/thinktank/en/document/EPRS_BRI.
- Hao, S., Ren, S., Zhou, N., Chen, H., Usman, M., He, C., Shi, Q., Luo, G., Zhang, S., 2020. Molecular composition of hydrothermal liquefaction wastewater from sewage sludge and its transformation during anaerobic digestion. *J. Hazard Mater.* 383, 121163 <https://doi.org/10.1016/j.jhazmat.2019.121163>.
- Her, N., Amy, G., McKnight, D., Sohn, J., Yoon, Y., 2003. Characterization of DOM as a function of MW by fluorescence EEM and HPLC-SEC using UVA, DOC, and fluorescence detection. *Water Res.* 37, 4295–4303. [https://doi.org/10.1016/S0043-1354\(03\)00317-8](https://doi.org/10.1016/S0043-1354(03)00317-8).
- Hidalgo, F.J., Alaiz, M., Zamora, R., 1999. Effect of pH and temperature on comparative nonenzymatic browning of proteins produced by oxidized lipids and carbohydrates. *J. Agric. Food Chem.* 47, 742–747. <https://doi.org/10.1021/jf980732z>.
- Ifon, B.E., Adyari, B., Hou, L., Zhang, L., Liao, X., Peter, P.O., Rashid, A., Yu, C.P., Hu, A., 2023. Insight into variation and controlling factors of dissolved organic matter between urban rivers undergoing different anthropogenic influences. *J. Environ. Manag.* 326 <https://doi.org/10.1016/j.jenvman.2022.116737>.
- Ignatev, A., Tuhkanen, T., 2019. Step-by-step analysis of drinking water treatment trains using size-exclusion chromatography to fingerprint and track protein-like and humic/fulvic-like fractions of dissolved organic matter. *Environ. Sci. Water Res. Technol.* 5, 1568–1581. <https://doi.org/10.1039/c9ew00340a>.
- Kaşanin-Grubin, M., Štrbac, S., Antonijević, S., Djogo Mračević, S., Randjelović, D., Orlić, J., Šajnović, A., 2019. Future environmental challenges of the urban protected area Great War Island (Belgrade, Serbia) based on valuation of the pollution status and ecosystem services. *J. Environ. Manag.* 251 <https://doi.org/10.1016/j.jenvman.2019.109574>.
- Lee, S., Park, J., 2022. Identification of dissolved organic matter origin using molecular level analysis methods. *Water (Switzerland)* 14, 1–10. <https://doi.org/10.3390/w14091317>.
- Leenheer, J.A., Croue, J.P., 2003. Characterizing aquatic dissolved organic matter. *Environ. Sci. Technol.* 37, 18A–26A. <https://doi.org/10.1021/es032333c>.
- Linnik, P., Osadchyi, V., Osadcha, N., 2023. Photochemical processes in surface water bodies and their potential impacts on the chemical composition of water: a review. *Lakes Reserv. Sci. Policy Manag. Sustain. Use.* 28, 1–15. <https://doi.org/10.1111/lre.12436>.
- Lu, D., Le, C., Zhou, Y., 2019. Identification of recalcitrant compounds after anaerobic digestion with various sludge pretreatment methods. *Post Treat. Anaerobically Treat. Effluents*. https://doi.org/10.2166/9781780409740_0283, 0.
- Ma, H., Allen, H.E., Yin, Y., 2001. Characterization of isolated fractions of dissolved organic matter from natural waters and a wastewater effluent. *Water Res.* 35, 985–996. [https://doi.org/10.1016/S0043-1354\(00\)00350-X](https://doi.org/10.1016/S0043-1354(00)00350-X).
- McDowell, W.H., 2023. DOM in the long arc of environmental science: looking back and thinking ahead. *Biogeochemistry* 164, 15–27. <https://doi.org/10.1007/s10533-022-00924-w>.
- Mohsin, G.F., Schmitt, F.J., Kanzler, C., Dirk Epping, J., Flemig, S., Hornemann, A., 2018. Structural characterization of melanoidin formed from D-glucose and L-alanine at different temperatures applying FTIR, NMR, EPR, and MALDI-ToF-MS. *Food Chem* 245, 761–767. <https://doi.org/10.1016/j.foodchem.2017.11.115>.
- Mohsin, G.F., Schmitt, F.J., Kanzler, C., Hoehl, A., Hornemann, A., 2019. PCA-based identification and differentiation of FTIR data from model melanoidins with specific molecular compositions. *Food Chem* 281, 106–113. <https://doi.org/10.1016/j.foodchem.2018.12.054>.
- Nabaterega, R., Kumar, V., Khoei, S., Eskicioglu, C., 2021. A review on two-stage anaerobic digestion options for optimizing municipal wastewater sludge treatment process. *J. Environ. Chem. Eng.* 9 <https://doi.org/10.1016/j.jece.2021.105502>.
- Nebbioso, A., Piccolo, A., 2012. Advances in humeomics: enhanced structural identification of humic molecules after size fractionation of a soil humic acid. *Anal. Chim. Acta.* 720, 77–90. <https://doi.org/10.1016/j.aca.2012.01.027>.
- Obileke, K.C., Nwokolo, N., Makaka, G., Mukumba, P., Onyeaka, H., 2021. Anaerobic digestion: Technology for biogas production as a source of renewable energy—a review. *Energy Environ.* 32, 191–225. <https://doi.org/10.1177/0958305X20923117>.
- Perminova, I.V., Frimmel, F.H., Kudryavtsev, A.V., Kulikova, N.A., Abbt-Braun, G., Hesse, S., Petrosyan, V.S., 2003. Molecular weight characteristics of humic substances from different environments as determined by size exclusion chromatography and their statistical evaluation. *Environ. Sci. Technol.* 37, 2477–2485. <https://doi.org/10.1021/es0258069>.
- Rajasulochana, P., Preethy, V., 2016. Comparison on efficiency of various techniques in treatment of waste and sewage water – a comprehensive review. *Resour. Technol.* 2, 175–184. <https://doi.org/10.1016/j.refit.2016.09.004>.
- Rodríguez, F.J., Schlenger, P., García-Valverde, M., 2014. A comprehensive structural evaluation of humic substances using several fluorescence techniques before and after ozonation. Part I: structural characterization of humic substances. *Sci. Total Environ.* 476–477, 718–730. <https://doi.org/10.1016/j.scitotenv.2013.11.150>.
- Rodríguez, E., García-Encina, P.A., Stams, A.J.M., Maphosa, F., Sousa, D.Z., 2015. Meta-omics approaches to understand and improve wastewater treatment systems. *Rev. Environ. Sci. Biotechnol.* 14, 385–406. <https://doi.org/10.1007/s11157-015-9370-x>.
- Rodríguez-Vidal, F.J., García-Valverde, M., Ortega-Azabache, B., González-Martínez, Á., Bellido-Fernández, A., 2020. Characterization of urban and industrial wastewaters using excitation-emission matrix (EEM) fluorescence: Searching for specific fingerprints. *J. Environ. Manag.* 263 <https://doi.org/10.1016/j.jenvman.2020.110396>.
- Rodríguez-Vidal, F.J., García-Valverde, M., Ortega-Azabache, B., González-Martínez, Á., Bellido-Fernández, A., 2021. Using excitation-emission matrix fluorescence to evaluate the performance of water treatment plants for dissolved organic matter removal. *Spectrochim. Acta - Part A Mol. Biomol. Spectrosc.* 249 <https://doi.org/10.1016/j.saa.2020.119298>.
- Tatla, H.K., Ismail, S., Khan, M.A., Dhar, B.R., Gupta, R., 2024. Coupling hydrothermal liquefaction and anaerobic digestion for waste biomass valorization: a review in context of circular economy. *Chemosphere* 361. <https://doi.org/10.1016/j.chemosphere.2024.142419>.
- Usman, M., Ren, S., Ji, M., O-Thong, S., Qian, Y., Luo, G., Zhang, S., 2020. Characterization and biogas production potentials of aqueous phase produced from hydrothermal carbonization of biomass – major components and their binary mixtures. *Chem. Eng. J.* 388, 124201 <https://doi.org/10.1016/j.ccej.2020.124201>.
- Vogt, R.D., Porcal, P., Hejzlar, J., Paule-Mercado, M.C., Haaland, S., Gundersen, C.B., Orderud, G.I., Eikebrokk, B., 2023. Distinguishing between sources of natural dissolved organic matter (DOM) based on its characteristics. *Water (Switzerland)* 15. <https://doi.org/10.3390/w15163006>.
- Wang, H.Y., Qian, H., Yao, W.R., 2011. Melanoidins produced by the Maillard reaction: structure and biological activity. *Food Chem* 128, 573–584. <https://doi.org/10.1016/j.foodchem.2011.03.075>.
- Yu, M., Liu, S., Li, G., Zhang, H., Xi, B., Tian, Z., Zhang, Y., He, X., 2020. Municipal wastewater effluent influences dissolved organic matter quality and microbial community composition in an urbanized stream. *Sci. Total Environ.* 705 <https://doi.org/10.1016/j.scitotenv.2019.135952>.
- Zhang, H., Zheng, J., Wang, X.C., Wang, Y., Dzakpasu, M., 2021. Characterization and biogeochemical implications of dissolved organic matter in aquatic environments. *J. Environ. Manag.* 294, 113041 <https://doi.org/10.1016/j.jenvman.2021.113041>.
- Zhen, G., Lu, X., Kato, H., Zhao, Y., Li, Y.Y., 2017. Overview of pretreatment strategies for enhancing sewage sludge disintegration and subsequent anaerobic digestion: Current advances, full-scale application and future perspectives. *Renew. Sustain. Energy Rev.* 69, 559–577. <https://doi.org/10.1016/j.rser.2016.11.187>.
- Zheng, Y., He, W., Li, B., Hur, J., Guo, H., Li, X., 2020. Refractory humic-like substances: tracking environmental impacts of anthropogenic Groundwater Recharge. *Environ. Sci. Technol.* 54, 15778–15788. <https://doi.org/10.1021/acs.est.0c04561>.